INTERNATIONAL JOURNAL OF SCIENCE, TECHNOLOGY AND DESIGN

ULUSLARARASI
BİLİM, TEKNOLOJİ VE TASARIM DERGİSİ

ISSN: 2757-8127, http://uludag.edu.tr/istd

The Physical Properties of CZTS Absorber Layer for Solar Cell Application

Serhat SARSICI[1], Hüseyin Kaan KAPLAN[2], Ali OLKUN[3], Reza MOHAMMADİGHAREHBAGH[4], Sertan Kemal AKAY[5]

[1] *Bursa Uludag University, Arts and Science Faculty,Department of Physics, Bursa, TURKEY, ORCID ID 0000-0003-1288-0431*
[2] *Bursa Uludag University, Arts and Science Faculty,Department of Physics, Bursa, TURKEY, ORCID ID 0000-0002-4144-5837*
[3] *Bursa Uludag University, Arts and Science Faculty,Department of Physics, Bursa, TURKEY, ORCID ID 0000-0003-0061-0573*
[4] *Bursa Uludag University, Arts and Science Faculty,Department of Physics, Bursa, TURKEY, ORCID ID 0000-0002-0333-487X*
[5] *Bursa Uludag University, Arts and Science Faculty,Department of Physics, Bursa, TURKEY, ORCID ID 0000-0002-7597-1528*

Corresponding Author: serhatsarsici@uludag.edu.tr,

Abstract

In this research, the Kesterite structure CZTS absorber layer was deposited on the glass substrate using a vacuum thermal evaporation technique. The morphological, electrical, structural, and optical properties of the produced films were examined utilizing Atomic Force Microscopy, Hall Effect Measurement system, Raman spectroscopy, and UV-Vis spectrophotometer measurements. The Raman analysis confirms the domination of Kesterite phase CZTS on the glass substrate, while secondary and ternary phases are also detected. According to the optical results, the optical bandgap value was calculated as 1.46 eV. The film's electric resistivity was measured as about 67 and 331 Ω.cm at 1 and 100 nA currents, respectively. The carrier concentration values were similarly calculated at 10^{15} cm^{-3} for 1 and 100 nA, respectively. Regarding the surface analysis, the RMS roughness value of the film is measured as approximately 5 nm. The RMS roughness and optical bandgap values illustrate the excellent morphological distribution and optical properties and proved that the used deposition technique is one of the best methods.

Article Info

Research Article
Received: 27/12/2020
Accepted: 26/01/2021

Keywords

CZTS, Solar cell, Physical properties, Absorber layer

Highlights

Alternative semiconductor to increase the efficiency of solar cells, alternative absorbent layer, More readily available and non-toxic elements, CZTS and secondary phase

Güneş Pili Uygulaması için CZTS Soğurucu Tabakanın Fiziksel Özellikleri

Özet

Bu araştırmada, Kesterit yapılı CZTS soğurucu tabaka cam alttaş üzerine vakum termal buharlaştırma tekniği ile biriktirilmiştir. Üretilen filmin morfolojik, elektriksel, yapısal ve optik özellikleri sırasıyla Atomik Kuvvet Mikroskobu, Hall Etkisi Ölçüm sistemi, Raman spektroskopisi ve UV-Vis spektrofotometre ölçümleri ile incelenmiştir. Raman analizi, Kesterit fazı CZTS'nin cam alttaş üzerindeki baskınlığını doğrularken, ikincil ve üçlü fazlar da tespit edilmiştir. Optik sonuçlara göre optik yasak enerji bant aralığı değeri 1.46 eV olarak hesaplanmıştır. Filmin elektriksel karakteristiği 1 ve 100 nA'da sırasıyla yaklaşık 67 ve 331 Ω.cm direnç göstermiştir. Taşıyıcı konsantrasyon değerleri, sırasıyla 1 ve 100 nA için benzer şekilde 10^{15} cm^{-3} mertebesinde ölçülmüştür. RMS pürüzlülüğü ve optik bant aralığı değerleri, mükemmel morfolojik dağılım ve optik özellikler göstermiştir ve kullanılan biriktirme tekniğinin diğerleri arasında en iyi tekniklerden biri oluğunu kanıtlamıştır.

Anahtar Kelimeler

CZTS, Güneş hücre, Fiziksel özellikler, Soğurucu katman

Öne Çıkanlar

Güneş pillerinin verimliliğini arttırmak için alternatif yarı iletken, alternatif soğurucu katman, Daha kolay bulunabilir ve toksik olmayan elementler,CZTS ikincil faz

1. Introduction

An increasing need for energy in the world, especially in recent years and exhausted, limited and become more expensive day by day in a fossil fuels-based resources fact over time cause to move toward alternative renewable energy resources. Besides, benefiting from endless solar energy with photovoltaic (PV) device is a promising candidate. Also, solar energy is the most natural and environmentally friendly alternative resource compared to non-renewable energy sources. When solar energy and fossil fuels are compared in terms of energy potential, the following result emerges. Even though fossil fuel reserves are limited and exhausted, even the energy reaching the earth from the sun in just 1 hour is sufficient to meet humanity's energy needs for a year [1].

One way of directly converting solar energy into electricity is using a semiconductor device called a solar cell. This phenomenon is well-known as the PV effect. The fundamental process (means work mechanism of the solar cell) behind this vital effect is based on the generation of electron-hole pairs through absorption of visible or electromagnetic radiation emitted from the sun via semiconductor devices. Using absorber materials that are p-type semiconductors play an important role in this process. According to the literature review, using various types of semiconductor materials as solar cells have some negative consequences that need urgent improvement. Meanwhile,

the upcoming and desired solar cells are as low-cost and highly efficient as possible. Under these conditions, it can simply reduce the human demand for traditional energy sources, increase the attention to solar cells, and find a definitive solution to humanity's energy needs. Besides, the solar cells can be attractive to both the consumer and the manufacturer. On this road, production costs can also be reduced, thereby using less material and less space notwithstanding the fact that the fabricated thin-film solar cells do not come close to the efficiency of traditional silicon single crystal solar cells. In comparison, these thin-films can be produced in smaller sizes and provide cheaper production with less raw material, leading to increased interest in thin-film solar cells [2].

As a thin film absorber material, there are three preferred categories that have been studied for many years. The first choices compared to other conventional single crystal silicon are cadmium telluride (CdTe), copper indium gallium diselenide ($CuInSe_2$ or CIGS), and amorphous thin-film silicon (a-Si). Among them, CdTe and CIGS solar cells are the leading commercialized thin-film solar cells. Some of the CIGS and CdTe based solar cell studies have approached about 22% efficiency in the laboratory environment. The module efficiency has reached 17%, which can compete with a-Si based solar cells [2]. Despite the advantages and the superior properties of CdTe and CIGS thin films, these classes of materials are some disadvantages. For instance, Te and In elements are rare and expensive; besides, Cd and Se elements are toxic. Today, these elements are mostly used in solar cell systems with high efficiency. Studies based on abundant and non-toxic elements include thin-film solar cells are still strongly ongoing. Due to the abundance, non-toxicity, low-cost elements exist in its structure, and suitable optical properties, Cu_2ZnSnS_4 (CZTS), $Cu_2ZnSnSe_4$ (CZTSe), and $Cu_2ZnSn\ (SSe)_4$ (CZTSSe) structures show promising for thin-film solar cell applications in recent years [3]. As an optical view, the CZTS semiconductor has a direct optical bandgap. By varying the sulfur and selenium content in the CZTSe layer, the optical bandgap can vary between 1.0 and 1.5 eV [4]. Based on various reports, the best bandgap value for this type of semiconductor thin film is found to 1.35 eV, which provides us high efficiency solar cells and allows the solar spectrum to be used in the best way [5]. In this semiconductor structure, obtaining an optical bandgap close to 1.35eV and an absorption coefficient higher than 10^4 cm^{-1} ensures effective absorption of photons [6]. Regarding the features mentioned above, CZTS based solar cell applications have attracted more interest from the research groups day by day. Various research groups have used several methods such as magnetron sputtering [7], sol-gel, electron beam evaporation [8], spray pyrolysis [9], etc., in recent years for the deposition of high-quality CZTS thin films.

In this work, the CZTS absorbent layer coated onto the glass substrate using the vacuum thermal evaporation technique. The morphological, optical, electrical, and structural characteristics of the deposited films have been analyzed through atomic force microscopy (AFM), UV-Vis spectrophotometer, Hall-effect, and Raman spectroscopy measurements, respectively.

2. Material and Method

In this process, the first step is preparing desired powders, then CuS, Sn, ZnS powders with 99.95+%, 99.9%, and 99.99% purities, and glass as substrate selected as starting

materials. The used elements' weight ratio has been arranged as %35 Cu, %15 Zn, %25 Sn, and %25 S. Afterward, the pellets of mixed powders were prepared using a 15 tons desktop hydraulic press combined with 13 mm dia pellet die. Before deposition, the substrate passed within the different cleaning processes to reach a clean and dust-free surface. The cleaning processes are rinsed in DI water, Acetone, and finally Ethanol for 5 minutes, respectively. Rinsing in the Acetone and ethanol has been carried out inside the ultrasonic bath cleaner. The overall procedure has been completed after washing the substrate using Alcohol for removing any undesired dirt and then leaves it to dry at the room temperature environment.

The second process was taking the place of the cleaned glass substrate into the substrate holder inside the vacuum chamber. Also, the pelletized powders were placed in the boat made of Mo element. All deposition processes performed using the vacuum thermal evaporation technique. So, the vacuum chamber closed, and the evacuation route started. The vacuum procedure initially starts with mechanical and then continues with diffusion pumps to achieve the pressure under 10^{-5} Torr. All the deposition parameters, such as base pressure, thickness, deposition rate, and substrate rotation speed, were recorded via computer. The deposition rate and the film thickness value monitored and controlled through in-situ quartz crystal microbalance (QCM) instruments during the coating process. The substrate holder's rotation speed kept constant at 9 RPM during the deposition of CZTS thin-films.

In the three and final step, the CZTS pellet's evaporation was performed by heating the pellet with the vacuum evaporation unit's manually controlled power source. The power was gradually increased to heat up the boat source to outgas gently. The purpose of this was to prevent the pellet pop-off from the boat source due to sudden evaporation due to sudden heating and to avoid inhomogeneities in the film by precisely controlling the deposition rate.

3. Results and Discussion

3.1. Raman Spectroscopy

The microscopic nature of the structural and/or morphological disorder, vibrational properties, sample quality, lattice dynamics, and impurities incorporation in the coated CZTS films. It was noticed that the technique is non-destructive and so sensitive. In our case, the Raman measurement has been carried out between 100 and 500 cm^{-1} range and illustrated in figure 1. According to the Raman spectra, four intense peak centers have been seen, which are sorted as 289, 219, 208, 338, 368, and 120 cm^{-1}, respectively. Overall, the spectrum, the most intense peak, emerged as 289 cm^{-1} assigned as A_{1g} mode of Kesterite CZTS [10]. The peak at 219 cm^{-1} is identified as the primary vibrational mode of the SnS phase in the structure [11]. The peaks centered at 338 [12] and 368 cm^{-1} [13] are attributed to A_1 and B_1 modes of the quaternary Kesterite phase of CZTS, respectively. These findings are in good consistency with research reported by authors [14]. As can be easily seen, in our case, the dominant peaks are detected at 289 and 338 $cm^{-1,}$ thereby referred to the vibration of the sulfur atom in the CZTS structure accordingly.

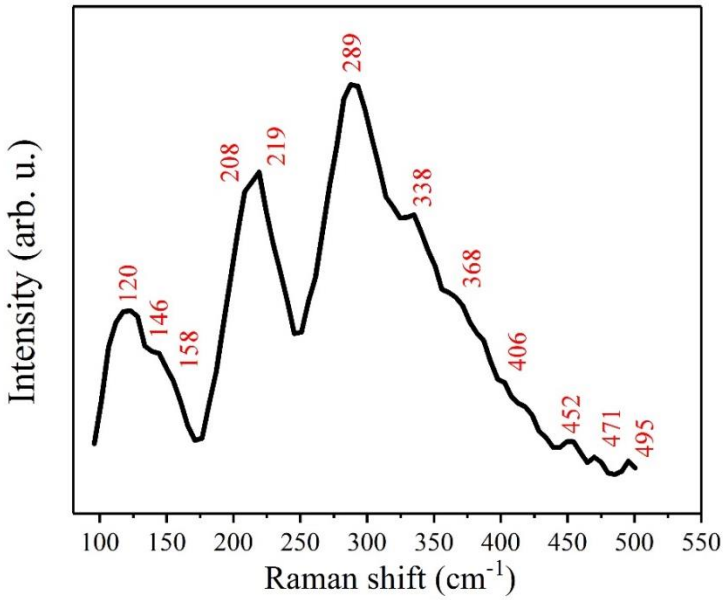

Figure 1. The Raman spectra of the CZTS film deposited on the glass substrate

Some low-intensity centers were also observed in addition to the previous peaks, such as 146, 406, 158, 471, and 495 $cm^{-1,}$ to their intensities in this spectrum. Thus, the peaks at 146 cm^{-1} are defined as the E (LO) mode of the Kesterite structure of CZTS [15]. But the peaks obtained at 158, 471, and 495 cm^{-1} confirm the existence of secondary phases, that is, SnS, $Cu_{2-x}S$, and Cu_xS, respectively [16]. Finally, the peak located at 406 cm^{-1} giving rise to background noise due to used Raman device; the same condition already reported by J. Ge et al. [11].

3.2. UV-Vis Spectrophotometer

The optical properties of the prepared absorber films were measured using a UV-Vis spectrophotometer. The absorbance (A) and transmittance (T) features versus wavelength of the thin-films were plotted in Figure 2. In the figure, the absorbance curve fluctuation between 200-400 nm of the film is concluded by the glass substrate. In this curve also an abrupt change in both transmittance and absorbance can be fluently seen. Two shoulders have been perceived in the transmittance curve that might be pertaining to secondary phases identified by Raman spectroscopy.

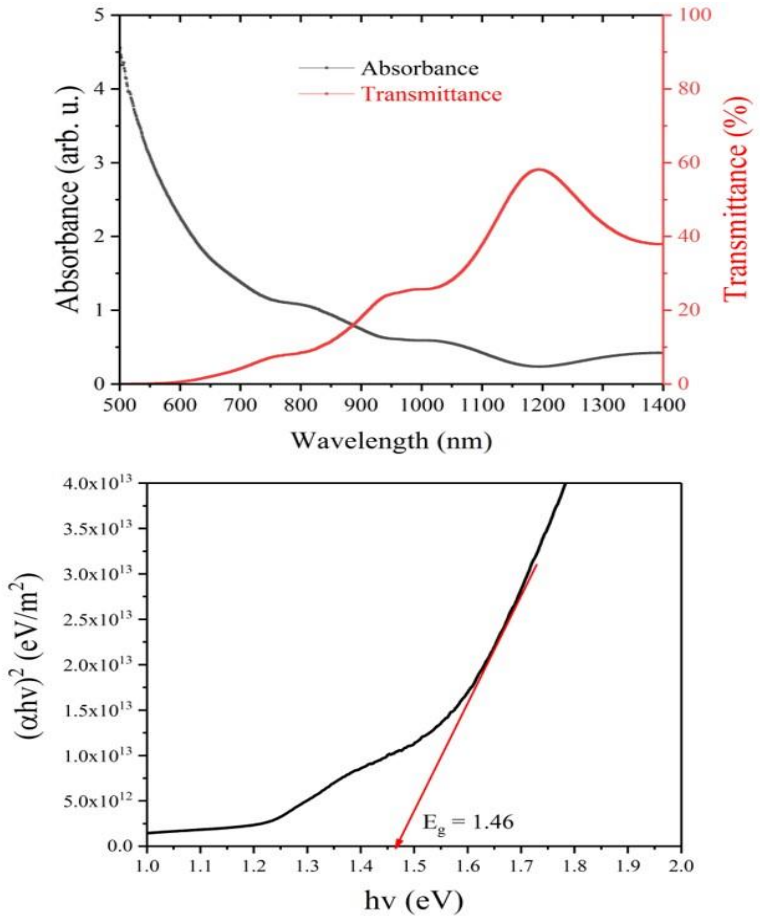

Figure 2. The absorbance and transmittance curves of the film (up) and the optical bandgap of the CZTS film (bottom)

In this measurement, the optical bandgap value (E_g) of the produced films calculated by obeying the well-known Tauc formula:

$$\alpha h\nu = B(h\nu - E_g)^m \quad (1)$$

Herein the B is a constant, h is the Planck's constant, $h\nu$ is photon energy, and α is an absorption coefficient that computed according to the below formula:

$$\alpha = 2.303\,(A/t) \quad (2)$$

where t is the standpoint of the thickness of the films, which was recorded as 520 nm. In the Tauc formula, m is a demonstration of the transition of the materials and are 2, 1/2, and 3/2 values; in our case, m is equal to 1/2 shows the allowed direct nature of the film. This value is strongly related to the electronic properties of the films. The value was 1.46 eV in the given spectra for deposited CZTS film on the glass substrate. This value is so close to the calculated optimum absorber layer E_g value, nearly similar to other researchers for CZTS film [17,18]. This finding is confirming the formation of CZTS and is in good consistent with Raman measurement.

3.3. Hall Effect Measurement

One of the essential properties of the film is its electronic characteristics. The Hall Effect (HMS 3000) measurements were performed to reveal the film's various electronic parameters. All measurements were run in room-temperature conditions by obeying a van der Pauw configuration under a 0.556 T magnetic field. In this analysis, the carrier concentration, Hall mobility, and sheet concentration of the film were obtained by 1.28×1015 cm-3, 72.7 $cm^2/V·s$, and $6.68×10^{10}$ cm-2, respectively at 1 nA current. Furthermore, the resistivity and conductivity of the same film noted by 67 Ω·cm and $1.49×10^{-2}$ 1/Ω·cm, respectively. The mentioned parameters are recorded as $6.83×10^{15}$ cm^{-3}, 2.76 $cm^2/V·s$, and $3.55×10^{11}$ cm^{-2} by keeping a similar condition at 100 nA. For this current value, the film's resistivity and conductivity are registered as 331 Ω and $3.02×10^{-3}$ 1/Ω·cm, respectively. It is clearly seen that the increase in current value causes a subsequent increase in the film's resistivity values. In light of the carrier concentration view, the same increase in the value can be depicted. Under the electric characterization, the p-type conductivity and ohmic behavior of the CZTS film were revealed and illustrated in figure 3.

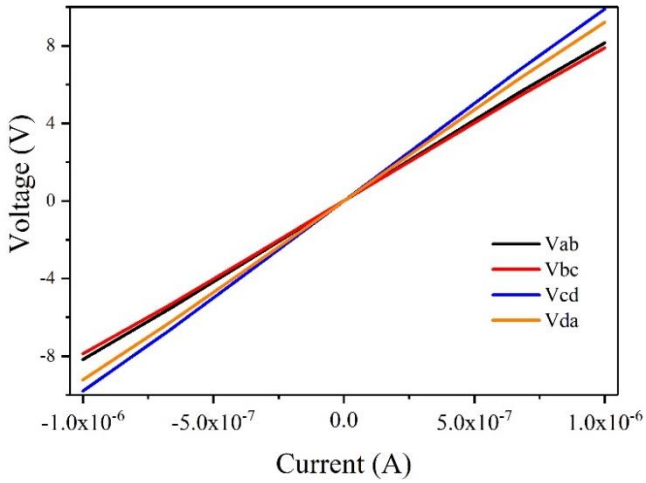

Figure 3. The current-voltage features of the deposited CZTS film on the glass substrate

3.4. Atomic Force Microscopy (AFM)

The deposited films' morphological properties on the glass substrate were investigated by utilizing the Atomic Force Microscopy (AFM). Essential morphological parameters such as average height, root-mean-square (RMS) roughness, Kurtosis, and Skewness of the films obtained from the AFM studies and given in Figure 4. In our CZTS film, the films' RMS roughness value was observed as approximately 5 nm, which gently inferred an excellent structural characteristic and charge transfer capacity. On the other hand, the average height was recorded as 4 nm. In this measurement, the roughness value is the more effective and crucial among them. According to the two-dimensional and three-dimensional figures, it is seen that the surface is fully covered by diverse height grains as well as valleys.

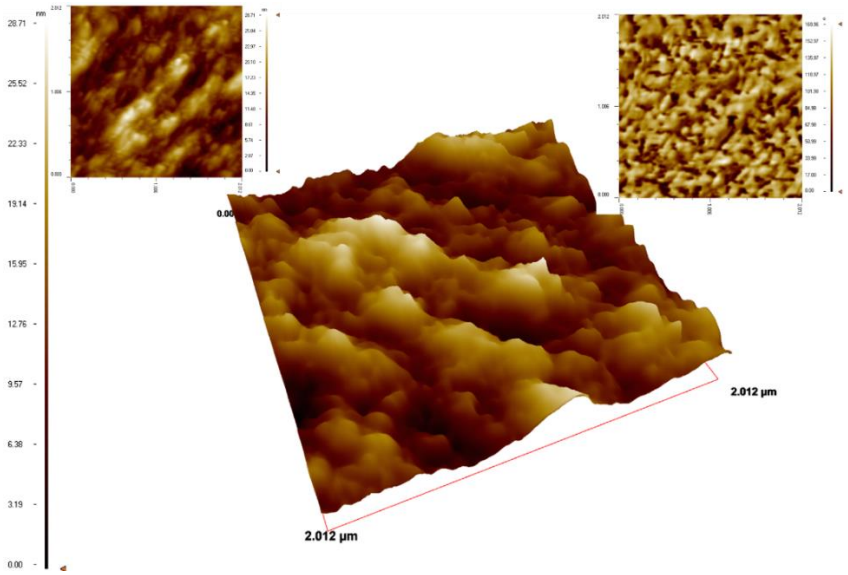

Figure 4. The two- and three-dimensional images of the CZTS film on the glass substrate

The Kurtosis and Skewness values show the distribution of the peak and valley upon or under the average line and symmetry of the grains distributed on the surface of the prepared film. In the produced CZTS film on the glass substrate, the parameters were found to be 2.9 and 0.34, respectively. Generally, the Kurtosis value of lower than 3 indicates a bumpy surface, the approaching of the value to 3 affirmation of random direction surface [19]. The Skewness is strongly affected by maximum peaks and the lowest valleys on the surface. The positive value of the Skewness evokes capacity when load takes place and porosity [20].

4. Conclusion

CZTS thin film was successfully grown onto a glass substrate using the vacuum thermal evaporation technique. The thickness of the thin film was measured at 520 nm. Raman analysis results showed that CZTS phases are dominant, but secondary and ternary phases are also present in the structure. The surface images show the homogenous, dense, compact, and smooth distribution of the grains on the substrate by consideration of morphological results. This distribution paved the way for utilizing the CZTS layer in solar cell configuration as well as pertaining to the good structural quality of the film. UV-Vis measurements showed that the thin film has high absorbance in the optical region. It was concluded that there is almost zero percent transmittance for photons with 200-700 nm. The energy band gap was calculated as 1.46 eV. While calculating the forbidden energy bandgap, it was observed that there were different linear regions. This supports the Raman analysis results. Electrical measurement results showed that the p-type semiconductor was produced, and the thin film had a carrier concentration of 1.28×10^{15} cm^{-3}. When the results were evaluated, it was seen that there could be an alternative and cheaper way to provide Sn additive in the production of CZTS thin film. It is concluded that it can be preferred as an absorber material for high energy photon applications, but its properties should be improved for solar cell applications. In future

studies, it is planned to improve the physical properties of CZTS thin film by changing the stoichiometry, adding different elements, increasing the coating thickness, producing different coating ratios and annealing in sulfur environment.

Financial support

No financial support has been received for the study.

Conflict of Interest

There is no conflict of interest.

Author Contribution

Each participant has an equal share.

5. References

Aslan, F., Tumbul, A. 2014. Non-vacuum processed Cu_2ZnSnS_4 thin films: influence of copper precursor on structural, optical and morphological properties. Journal of alloys and compounds 612: 1-4.

Chen, S., Gong, X. G., Walsh, A., Wei, S. H. 2010. Defect physics of the kesterite thin-film solar cell absorber Cu_2ZnSnS_4. Applied Physics Letters 96(2): 021902.

Dumcenco, D., Huang, Y. S. 2013. The vibrational properties study of kesterite Cu_2ZnSnS_4 single crystals by using polarization dependent Raman spectroscopy. Optical Materials 35(3): 419-425.

Friedlmeier, T. M., Wieser, N., Walter, T., Dittrich, H., Schock, H. 1997. Heterojunctions based on Cu_2ZnSnS_4 and $Cu_2ZnSnSe_4$ thin films. Proceedings of the 14th European Conference of Photovoltaic Science and Engineering and Exhibition.

Ge, J., Chu, J., Jiang, J., Yan Y., Yang, P. 2014. Characteristics of In-substituted CZTS thin film and bifacial solar cell. ACS applied materials & interfaces 6(23): 21118-21130.

Green, M. A., Emery, K., Hishikawa, Y., Warta, W. 2010. Solar cell efficiency tables (version 37). Progress in photovoltaics: research and applications 1(19): 84-92.

Haddout, A., Fahoume, M., Qachaou, A., Raidou, A., Lharch, M., Elharfaoui, N. 2019. Influence of composition ratio on the performances of kesterite solar cell with double CZTS layers—A numerical approach. Solar Energy 189: 491-502.

Ito, K., Nakazawa, T. 1988. Electrical and optical properties of stannite-type quaternary semiconductor thin films. Japanese Journal of Applied Physics 27(11R): 2094.

Jimbo, K., Kimura, R., Kamimura, T., Yamada, S., Maw, W. S., Araki, H., Oishi, K., Katagiri, H. 2007. Cu_2ZnSnS_4-type thin film solar cells using abundant materials. Thin solid films 515(15): 5997-5999.

Katagiri, H., Saitoh, K., Washio, T., Shinohara, H., Kurumadani, T., Miyajima, S. 2001. Development of thin film solar cell based on Cu_2ZnSnS_4 thin films. Solar Energy Materials and Solar Cells 65(1-4): 141-148.

Khemiri, N., Chamekh, S., Kanzari, M. 2020. Properties of thermally evaporated CZTS thin films and numerical simulation of earth abundant and non toxic CZTS/Zn (S, O) based solar cells. Solar Energy 207: 496-502.

Kumar, B. R., Rao, T. S. 2012. AFM studies on surface morphology, topography and texture of nanostructured zinc aluminum oxide thin films. Digest Journal of Nanomaterials and Biostructures 7(4): 1881-1889.

Mohammadigharehbagh, R., Pat, S., Akkurt, N., Olkun, A., Ozgur, M., Demirkol, U., Özen, S., Korkmaz, Ş. 2020. Surface, optical and electrochemical performance of indium-doped ZnO/WO_3 nano-composite thin films. SN Applied Sciences 2(11): 1-11.

Peksu, E., Terlemezoglu, M., Parlak, M., Karaagac, H. 2019. Characterization of one-step deposited Cu_2ZnSnS_4 thin films derived from a single crystalline powder. Renewable Energy 143: 1133-1142.

Persson, C. 2010. Electronic and optical properties of Cu_2ZnSnS_4 and $Cu_2ZnSnSe_4$. Journal of Applied Physics 107(5): 053710.

Prabeesh, P., Saritha, P., Selvam, I. P., Potty, S. 2017. Fabrication of CZTS thin films by dip coating technique for solar cell applications. Materials Research Bulletin 86: 295-301.

Scragg, J. J., Dale, P. J., Peter, L. M. 2008. Towards sustainable materials for solar energy conversion: Preparation and photoelectrochemical characterization of Cu_2ZnSnS_4. Electrochemistry Communications 10(4): 639-642.

Semenenko, M. O., Babichuk, I. S., Kyriienko, O., Bodnar, I. V., Caballero, R., Leon, M. 2017. RF electromagnetic field treatment of tetragonal kesterite CZTSSe light absorbers. Nanoscale Research Letters 12(1): 1-8.

Tanaka, K., Moritake, N., Uchiki, H., 2007. Preparation of Cu_2ZnSnS_4 thin films by sulfurizing sol–gel deposited precursors. Solar Energy Materials and Solar Cells 91(13): 1199-1201.

Tumbul, A., Aslan, F., Göktaş, A., Mutlu, I. 2019. All solution processed superstrate type Cu_2ZnSnS_4 (CZTS) thin film solar cell: effect of absorber layer thickness. Journal of Alloys and Compounds 781: 280-288.